 ©2011 Kvantovaya Elektronika and Turpion Ltd

PACS numbers: 87.16.dp; 79.20.Eb; 87.64.Cc; 87.80.Dj
DOI: 10.1070/QE2011v041n05ABEH014639

Fractional laser microablation of skin aimed at enhancing its permeability for nanoparticles

E.A. Genina, L.E. Dolotov, A.N. Bashkatov, G.S. Terentyuk, G.N. Maslyakova, E.A. Zubkina, V.V. Tuchin, I.V. Yaroslavsky, G.B. Altshuler

***Abstract*. A new method for delivering nanoparticles into the skin using the fractional laser microablation of its surface and the ultrasonic treatment is proposed. As a result of *in vitro* and *in vivo* studies, it is shown that the 290-nm laser pulses with the energy from 0.5 to 3.0 J provide the penetration of nanoparticles of titanium dioxide with the diameter $\sim$ 100 nm from the skin surface to the depth, varying from 150 to 400 μm. Histological testing of the skin areas, subjected to the treatment, shows that the particles stay in the dermis at the depth up to 400 μm no less than for three weeks.**

Keywords: *titanium dioxide, fractional laser microablation, ultrasonic treatment, reflectance spectroscopy, optical coherence tomography*.

1. Introduction

At present the diagnostic and therapeutic technologies, exploiting micro- and nanoparticles and widely used in medicine, remain a subject of intense research. Among multiple studies, devoted to transportation of nanoparticles in cells and various biological tissues, an important problem is how to insert the nanoparticles into the skin. Thus, for example, the nanoparticles of titanium dioxide, zinc oxide and gold are widely used as contrast agents for optical coherence tomography (OCT) [1, 2] and multiphoton tomography [3, 4] of skin. Gold and silver nanoparticles may be used as contrast agents for the cell visualisation [5, 6]. To protect the skin from UV radiation, the photoprotective preparations with the admixture of TiO_2 and ZnO nanoparticles are inserted into the surface layers of skin [7, 8]. The authors of [9] proposed to use silicon nanoparticles for this purpose. Moreover, nanoparticles can serve as carriers of medicinal preparations under their transcutaneous administration [10]. Gold nanoparticles are used for photothermal treatment of neoplasms hidden inside a tissue layer [11, 12]. In papers [13, 14] for the TiO_2 and $Ag-SiO_2$ nanoparticles a phototoxic action on pathogenic microorganisms was demonstrated, caused by both the nanoparticles themselves and their combination with dyes.

The main advantage of transcutaneous administration of preparations including nanoparticles is that in this case the delivery is executed directly to the pathologically modified areas of the tissue [15], which is important in photothermal of photochemical therapy of near-surface pathologies (naturally, under the condition of previous visualisation of the target object). However, the natural protective barrier of the skin, i.e., the corneal layer, 5–20 μm thick, consisting of plane densely packed cells – corneocytes, merged into the lipid matrix [16], makes inserting the agents deep into the skin a rather difficult problem. The hydrophilic pores, transpiercing the epidermis, have the diameter less than 10 nm [15]. It is shown in [17] that the iron-based nanoparticles, whose size is comparable with that of the natural pore diameter, overcome the corneal layer and penetrate into the skin dermis through living epidermis. To deliver nanoparticles of greater size use is made of either the ducts of skin glands and hair follicles, having the diameter not less than 5 μm [15], or the artificial channels produced using sonoporation [18], electroporation [19] or microporation under the mechanical [2, 20] or optothermal action [21]. Nanoparticles are inserted in different ways, e.g., by infriction [3, 4, 22], by generation of photomechanical waves [23] or ultrasonic treatment [2], by needleless injection [24, 25]. It was shown that the depth of penetration of TiO_2 nanoparticles with the mean diameter $\sim$ 100 nm into the skin by infriction is $\sim$ 3 μm [22]. In this case nanoparticles penetrate into the skin only through the orifices of the hair follicles and the ducts of sweat and oil glands [26].

Creation of artificial channels by means of microporation promotes deeper and more targeted delivery of nanoparticles. In this case the diameter and the depth of pores depend on the instruments, acting on the skin [15]. Thus, if the diameter of the thinnest standard needle, available at present, is 184 μm, the diameters of microneedles, used in the mechanical microporation, may reach $\sim$ 100 μm, while the diameters of microchannels, created as a result of thermo- and electroporation, may be 10–50 μm [15, 19]. The mean depth of penetration of solid particles at needleless injection varies from less than 10 μm to more

E.A. Genina, L.E. Dolotov, A.N. Bashkatov, E.A. Zubkina, V.V. Tuchin Research and Educational Institute of Optics and Biophotonics, N.G. Chernyshevsky National Research Saratov State University, ul. Astrakhanskaya 83, 410012 Saratov, Russia; e-mail: eagenina@yandex.ru;
G.S. Terentyuk LLC 'The First Veterinary Clinic', ul. Astrakhanskaya 83, 410012 Saratov, Russia; e-mail: vetklinika@front.ru;
G.N. Maslyakova V.I. Razumovsky Saratov State Medical University, ul. Bol'shaya Kazach'ya 112, 410012 Saratov, Russia; e-mail: gmaslyakova@yandex.ru;
I.V. Yaroslavsky, G.B. Altshuler Palomar Medical Technology Inc., 82 Cambridge St. Burlington 01803 MA, USA

Received 4 April 2011
Kvantovaya Elektronika **41** (5) 396–401 (2011)
Translated by V.L. Derbov

than 20 μm [25]. The depth of nanoparticle delivery when using the mechanical microporation approaches 300 μm [2, 20].

Thus, the artificial microporation is the least invasive method used to insert micro- and nanoparticles into the skin at sufficiently large depth. In this case the sufficiently fast (during a few hours) restoration of the barrier integrity occurs after the injection of agents [18]. These specific features also reduce the risk of skin infection caused by the manipulations carried out [15].

Laser microablation (besides all advantages inherent in other microporation methods) allows the control not only of the depth, but also of the shape of the created microchannels by means of different attachments [27].

In the present paper we propose a new method of delivering nanoparticles into the skin at the depth up to 400 μm using the fractional laser microablation of the skin surface and the ultrasonic treatment.

2. Methods and materials

To overcome the protective skin barrier the technique of fractional laser microablation of the surface layers of epidermis was developed. The Palomar Lux2940 erbium laser (Palomar Medical Products Ltd., USA) was used as a light source. Its parameters were the following: the wavelength 2940 nm, the pulse energy 0.5 – 3.0 J. The pulses possessed a spike structure (from one to three spikes per pulse depending on the energy) with the spike duration of 200 μs. Two regimes of laser action were used in the experiments. In regime I, single-spike pulses with the energy ~ 1 J were used, while in regime II use was made of pulses with three spikes and energy ~ 3 J. The microchannels were produced by means of an attachment that allowed microablation of skin areas [27]. Five horizontal cuts were made in the skin on the area with the dimensions 5×5 mm (Figs 1a, b). The separation between the cuts was nearly 1.2 mm, the depth varied depending on the treatment regime. In regime I the depth of cuts was ~ 150 μm, in regime II it was nearly 300 μm (Figs 1c, d).

We used the TiO_2 nanopowder (634662-100G, Sigma-Aldrich Co., USA) consisting of a mixture of rutile and anatase titanium dioxide with the nanoparticle size less than 100 nm. To enhance the penetration into the skin and to suppress the photocatalytic action of photochemically active anatase form of TiO_2, the nanoparticles were suspended in polyethylene glycol having the molecular weight 300 (Sigma-Aldrich Co.). The concentration of nanoparticles in the suspension was 0.5 g mL^{-1}.

The suspension was prepared using the CT-400A ultrasonic bath (CTBrand, Wan Luen Electronic Tools Co. Ltd, China) with the radiation power of 35 W and the radiation frequency of 43 – 45 kHz. The cuvette with the suspension was placed into the ultrasonic bath for 30 min for thorough mixing of the content both in the process of preparation and directly before the use. The ultrasound was also used to enhance the penetration of the particles into the skin. It was generated by the Dinatron 125 ultrasonic transmitter (Dinatronics, USA) with the frequency 1 MHz and the power density 1.5 W cm^{-2} in the continuous regime.

The visualisation of microchannels, filled with the suspension of nanoparticles, was implemented using the Spectral Radar OCT System OCP930SR 022 (Thorlabs Inc., USA) at a wavelength of 930 nm.

The diffuse reflectance spectra were measured using the USB4000 multichannel spectrometer (Ocean Optics Inc., USA) in the spectral region 400 – 900 nm. The HL-2000 halogen lamp (Ocean Optics Inc., USA) served as a source of light. The QR400-7-VIZ/NIR fibreoptical probe (Ocean Optics Inc.) consisting of seven fibres with the internal

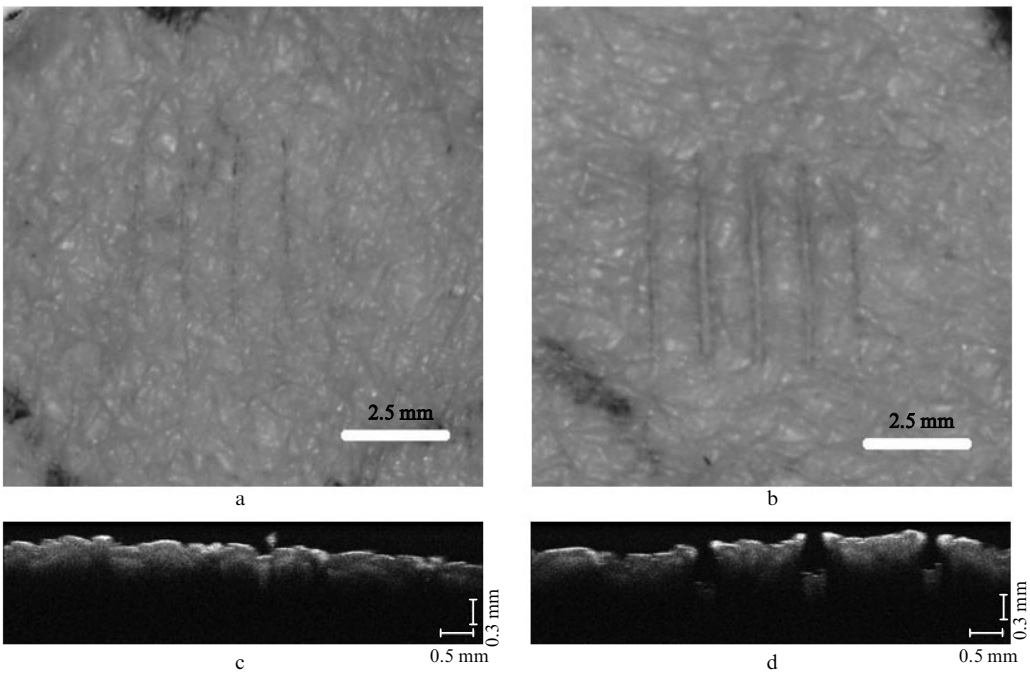

Figure 1. The result of laser radiation action on the skin *in vitro*: the skin surface after the laser fractional microablation by a single-spike pulse with the energy ~ 1 J (a) and a three-spiked pulse with the energy ~ 3 J (b); OCT images of the skin after the laser fractional microablation by a single-spike pulse (c) and a three-spiked pulse (d).

diameter 400 μm and the numerical aperture 0.2 was used in the measurements. The central fibre served for collecting the diffuse reflected radiation, while the surrounding six fibres were used for the illumination of the sample.

The probe was placed at the distance of 2 mm from the skin surface and registered the signal, averaged over the area of the radiation collection. The WS-1-SL reflectance standard (Ocean Optics Inc.) was used to normalise the reflectance spectra.

The *in vitro* experiments were carried out with four samples of human skin, taken out in the course of autopsy. The dimensions of the samples were approximately 1.0×1.0 cm, the average thickness 3.5 ± 0.2 mm. After the creation of microchannels the suspension of nanoparticles was applied to the studied areas of the skin. The total exposure time was 2 h. The ultrasonic treatment was performed periodically during all the exposure time, each period including 2 min of irradiation and a 13-minute pause. The summary time of the ultrasonic treatment was 16 min. During the procedure the sample was placed in a Petri dish with a small volume of saline (aqueous solution of NaCl with the concentration 0.9 mg mL^{-1}) to prevent the change in the optical properties due to dehydration. Then the suspension was removed from the skin surface with a tampon wetted with saline. The reminders of the suspension were removed using the Multi-film medical sticky tape (Tesa, Germany) by two surface strips. The mean thickness of each strip of epidermis was about 0.5 μm [22].

The measurements of the diffuse reflectance from the areas of skin and OCT scanning were performed before the insertion of nanoparticles and two hours after it.

The *in vivo* measurement of the transport of TiO_2 nanoparticles in the skin using the fractional laser microablation and ultrasonic treatment was carried out in LLC 'The First Veterinary Clinic' (Saratov, Russia). The subject of study was a Yucatan minipig male. The age of the animal was 2.5 months and the weight was 15 kg. A month before the experiment the studied area of skin was marked with a tattoo. The animal was anesthetised with the 2 % solution of xilasine (2 mL).

Before the beginning of the experiment the hair was removed from the studied skin area using the Nair depilatory cream (Church & Dwight Co., Inc., USA) and then the skin was disinfected with 90 % alcoholic solution. The solution of chlorhexidine in the proportion 3 : 2 was added to the suspension to prevent the infection of the target skin areas. The skin microablation was implemented using the laser pulses with the power 3 J (regime II) to provide deeper penetration of nanoparticles. To enhance the nanoparticle transport the treated areas were subjected to 15-minute ultrasonic treatment (3 min of irradiation alternating with 3-minute pauses). After the ablation and insertion of nanoparticles the suspension was removed from the studied areas of skin using distilled water. After the experiment the treated skin areas were covered by a bactericidal plaster. The observations were made during three weeks in the following sequence: two days, one, two and three weeks after the treatment. Each observation included skin surface photography using the Nikon D80 camera (Nikon Inc., Japan) with the Micro-Nikkor macro objective (Nikon Inc.).

Using the standard technique, the biopsy material was taken from the studied skin areas, located between the tattoo lines, and the histological sections were prepared. After fixation of the material with 10 % solution of formalin the samples were transferred through baths of progressively more concentrated ethanol to remove the water and then embedded in paraffin. Paraffined sections 6 – 8 μm thick were stained with haematoxylin and eosin.

The histological description of the preparations was carried out using the MC 100 XP microscope (Micros, Austria) operating in transmitted light with the magnification $200^{\times}$. Photographs were taken using the Canon PC 1107 camera (Canon Inc., Japan).

3. Results and discussion

Figure 2 presents the OCT-images of the skin samples *in vitro* before the treatment and after the fractional laser microablation and insertion of nanoparticles. The depth of probing is about 250 μm for the intact skin (Fig. 2a). In Figs 2b and 2c the microscopic cuts, created by microablation and filled with the nanoparticle suspension, are clearly seen (marked with arrows). The depth of penetration of nanoparticles coincides with that of the microscopic cuts. In the present case the depth of probing is reduced to 100 – 150 μm because of the screening of light by the layer of nanoparticles, kept at the bottom of the cuts and left on the skin surface.

Figure 3 shows the spectra of diffuse reflectance from the skin before and after the insertion of TiO_2 nanoparticles in the region of cuts at two ablation regimes. The solid curve corresponds to the reflection spectrum of the intact skin. The absorption bands of blood at the wavelengths 416 (Soret band), 543, and 578 nm are well seen. The dashed curve represents the spectrum of the same skin area after the microablation with a laser pulse with the energy ~ 1 J and the insertion of the suspension of nanoparticles (regime I). Since in this case the depth of microchannels did not exceed 150 μm, after the washing-off of the suspension and the surface stripping most particles were removed, but, apparently, not all of them. The change in the skin spectrum shape indicates the presence of some amount of TiO_2 nanoparticle suspension in the near-surface skin layers.

The reduction of the reflectance is most likely caused by the influence of the base substance of the suspension, polyethylene glycol PEG-300 that immerses the surface layer of the epidermis and, thus, reduces the value of the reflected signal. Besides that, while the thickness of the intact areas of skin was 3.5 ± 0.2 mm, the thickness of the ablated areas was essentially smaller, up to 2.8 ± 0.4 mm. This was caused by the enhanced dehydration of the biological tissue due to: (i) the enhanced evaporation of the intrstitial water from the skin dermis through the microchannels in the epidermis, and (ii) the effect of the hyperosmotic agent PEG-300, which, in turn, causes the osmotic dehydration of the skin dermis [28]. The reduction of the thickness of the tissue also promotes the decrease in its reflectance.

The dotted line in Fig. 3 corresponds to the reflection spectrum of the skin area after the microablation by laser pulses with the energy 3.0 J and insertion of nanoparticle suspension (regime II). In this case the depth of channels exceeded 300 μm; therefore, the suspension from the channels was not removed. Though the thickness of the sample decreased, the increase in the intensity of radiation reflected from the skin was observed, particularly in the range 400 – 500 nm, which is related to the substantial growth of the scattering coefficient of the tissue, promoted by the

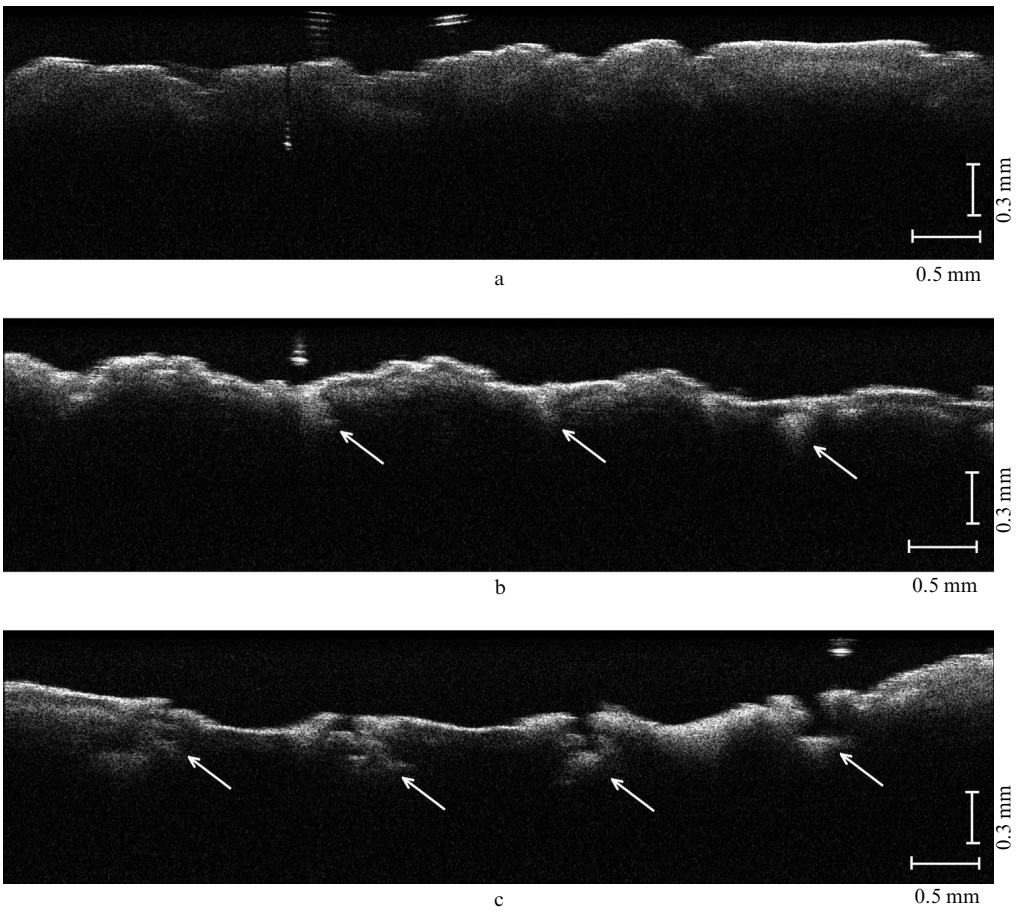

Figure 2. OCT-images of the human skin *in vitro*: the intact skin (a); the skin after microablation by a pulse with the energy ~ 1 J (b) and the pulse with the energy ~ 3 J (c) and insertion of TiO_2 nanoparticles. Arrows point at the areas of ablation.

nanoparticles located in the microchannels. The changes in the shape of the reflection spectrum confirm this evidence.

Figure 4 represents a series of photographs of the minipig skin areas before and after the insertion of nanoparticle suspension and ultrasonic treatment. In Figs 4b and 4c the microscopic cuts, filled with the titanium dioxide suspension, are easily seen at the crossings of the tattoo lines. Directly after the treatment on the animal skin one could observe erythema (Fig. 4b) that vanished during 15–20 min. Two days after the treatment (Fig. 4c) the complete healing of microchannels occurred and the peeling of the damaged surface layer of epidermis began. A week after the experiment the peeling finished and the integrity of the epidermis was restored (Fig. 4d). After 2–3 weeks the microscopic cuts were practically invisible; however, in the places of their location the tattoo contours were partially blurred (Fig. 4e) and the skin colour was slightly lightened (Fig. 4f, the lightened areas are marked with arrows).

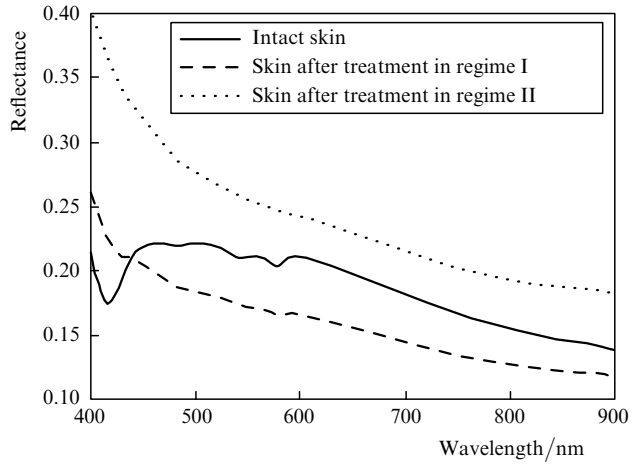

Figure 3. Spectra of diffuse reflectance of the skin *in vitro*: the solid curve corresponds to the spectrum of intact skin; the dashed curve represents the spectrum of the skin after the ablation by the pulse with the energy ~ 1 J and insertion of TiO_2 nanoparticles (regime I); the dotted curve represents the spectrum of the skin after the ablation by the pulse with the energy ~ 3 J and insertion of TiO_2 nanoparticles (regime II).

The effect of skin lightening may be explained by the presence of some part of nanoparticles that do not leave the skin as a result of the natural motion together with the epidermis cells towards the surface in the course of the cell division. After the restoration of the skin integrity the nanoparticles, inserted at the depth exceeding the epidermis thickness (100–150 μm), stay in the dermis, simulating a scattering screen, due to which the skin lightens.

This observation is confirmed by the results of the histological analysis. Histological sections allow observation of the nanoparticle localisation in the deep layers of the skin. In Fig. 5 the histological preparations, made of the biopsy material from the treated and control areas of skin are shown. TiO_2 nanoparticles, penetrated deep into the skin, are well seen in the photograph of the histological

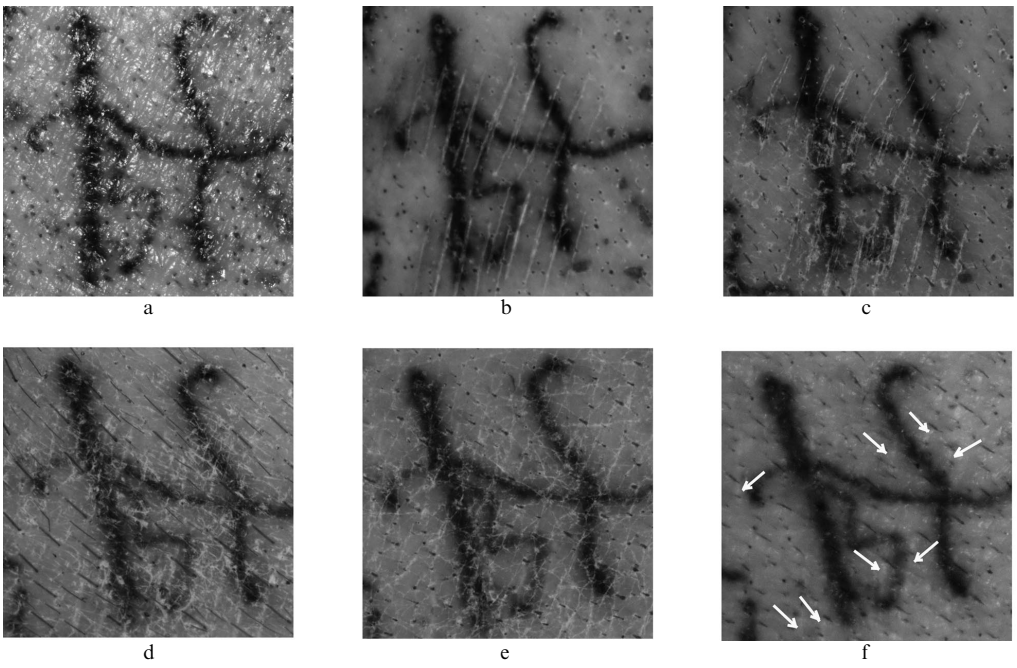

Figure 4. A series of photographs of the minipig skin areas, subjected to microablation and insertion of TiO_2 nanoparticles assisted with 15-minute ultrasonic irradiation: the intact skin (a); the skin view immediately after the treatment (b); two days (c); a week (d); two weeks (e); three weeks (f) after the treatment. The arrows point at the areas of lightened skin in the treated places.

sections (Fig. 5a, pointed by arrows). In the light transmission regime the clusters of particles look black against the background of the tissue image. The photograph allows estimation of the penetration depth that varied from 150 to 400 μm, which indicates the presence of the particles in the skin dermis. In the epidermis region no particles were detected. Moreover, the ultrasonic treatment, apparently, facilitated more uniform distribution of nanoparticles in the skin dermis. In the control region, located at some distance from the areas of microablation (Fig. 5b), the particles were not detected.

Thus, the variation in laser radiation parameters provided a variable depth of microchannels and, therefore, the controllable depth of nanoparticle insertion. Only in the case of deep insertion of the PEG-TiO_2 suspension the nanoparticles stayed inside the skin dermis during the entire period of observation (3 weeks). The results of observations showed that the erythema vanished from the areas of laser microablation during 15 – 20 min, and the complete healing of microchannels occurred during a week. The internal structure of the skin tissues in the treated areas was not disturbed.

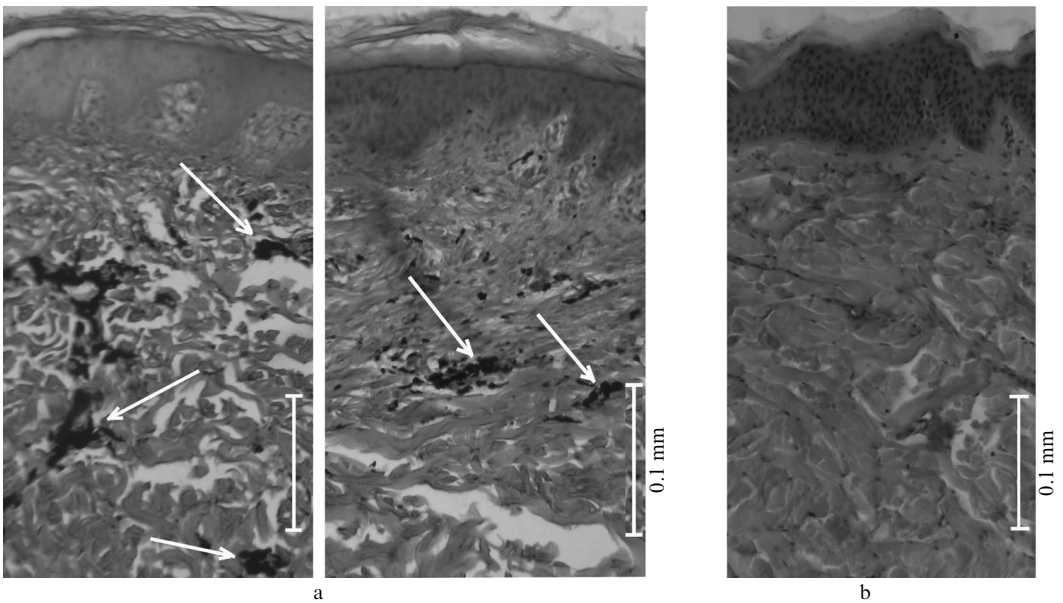

Figure 5. Photographs of histological preparations of the minipig skin biopsy three weeks after the microablation and insertion of TiO_2 nanoparticles into the skin (a); the control area (b). The preparations were stained with haematoxylin and eosin, the arrows point at the location of nanoparticles.

4. Conclusions

The performed research has shown that the use of fractional laser microablation allows efficient insertion of nanoparticles into the skin dermis. At the pulse energy ~ 3 J the microscopic cuts, created in the tissue by ablation, allowed nanoparticle insertion up to 400 μm deep into the dermis. Varying the pulse energy, one can change the cuts depth and, therefore, the depth of the particle delivery into the skin. Ultrasonic treatment facilitated the uniform filling of the microscopic cuts with the nanoparticle suspension and the distribution of nanoparticles in the dermis.

Deep insertion of nanoparticles allows them to stay in the dermis, which affects the optical characteristics of the skin (due to the enhancement of light scattering by the particles the reflectance increases and the skin lightens).

Acknowledgements. The authors express their gratitude to Palomar Medical Products Ltd. for financial support and equipment, to the staff of LLC 'The First Veterinary Clinic' for their help in work with animals. The work was carried out within the RF State Contracts (Nos 02.740.11.0484 and 02.740.11.0879).

References

1. Kirillin M., Shirmanova M., Sirotkina M., Bugrova M., Khlebtsov B., Zagaynova E. *J. Biomed. Opt*., **14**, 021017 (2009).
2. Kim C.S., Wilder-Smith P., Ahn Y.-C., Liaw L.-H., Chen Z., Kwon Y.J. *J. Biomed. Opt*., **14**, 034008 (2009).
3. Zvyagin A.V., Zhao X., Gierden A., Sanchez W., Ross J.A., Roberts M.S. *J. Biomed. Opt*., **13**, 064031 (2008).
4. Roberts M.S., Roberts M.J., Robertson T.A., Sanchez W., Thorling C., Zou Y., Zhao X., Becker W., Zvyagin A.V. *J. Biophotonics*, **1**, 478 (2008).
5. Schrand A.M., Braydich-Stolle L.K., Schlager J.J., Dai L., Hussain S.M. *Nanotechnology*, **19**, 235104 (2008).
6. Khanadeev V.A., Khlebtsov B.N., Staroverov S.A., Vidyasheva I.V., Skaptsov A.A., Ileneva E.S., Bogatyrev V.A., Dykman L.A., Khlebtsov N.G. *J. Biophotonics*, **4**, 74 (2011).
7. Edlich R.F., Winter K.L., Lim H.W., Cox M.J., Becker D.G., Horovitz J.H., Nichter L.S., Britt L.D., Long W.B. *J. Long-Term Effects Med. Implants*, **14**, 317 (2004).
8. Innes B., Tsuzuki T., Dawkins H., Dunlop J., Trotter G., Nearn M.R., McCormick P.G. *Cosmetics, Aerosols and Toiletries in Ausrtalia*, **15**, 21 (2002).
9. Rybaltovskii A.O., Bagratashvili V.N., Belogorokhov A.I., Koltashev V.V., Plotnichenko V.G., Popov A.P., Priezzhev A.V., Sviridova A.A., Zaitseva K.V., Tutorskii I.A., Ischenko A.A. *Opt. Spektrosk*., **101**, 626 (2006). [*Opt. Spectrosc*., **101**, 590 (2006)].
10. Kohli A.K., Alpar H.O. *Int. J. Pharm*., **275**, 13 (2004).
11. Huang X., Jain P.K., El-Sayed I.H., El-Sayed M.A. *Lasers Med. Sci*., **23**, 217 (2008).
12. Terentyuk G.S., Maslyakova G.N., Suleymanova L.V., Khlebtsov N.G., Khlebtsov B.N., Akchurin G.G., Maksimova I.L., Tuchin V.V. *J. Biomed. Opt*., **14**, 021016 (2009).
13. Tuchina E.S., Rudik D.V., Krylova G.V., Smirnova N.P., Eremenko A.M., Tuchin V.V. *Proc. SPIE Int. Soc. Opt. Eng*., **6163**, 61631V (2006).
14. Tuchina E.S., Tuchin V.V. *Laser Phys. Lett*., **7**, 607 (2010).
15. Cevc G., Vierl U. *J. Control. Release*, **141**, 277 (2010).
16. Schaefer H., Redelmeier T.E. *Skin Barrier* (Basel: Karger, 1996).
17. Baroli B., Ennas M.G., Loffredo F., Isola M., Pinna R., Lopez-Quintela M.A. *J. Invest. Dermatol*., **127**, 1701 (2007).
18. Tezel A., Sens A., Mitragotri S. *J. Control. Release*, **83**, 183 (2002).
19. Gowrishankar T.R., Pliquett U., Weaver J.C. *Ann. N.Y. Acad. Sci*., **888**, 183 (1999).
20. Roxhed N., Samel B., Nordquist L., Griss P., Stemme G. *IEEE Trans. Biomed. Eng*., **55**, 1063 (2008).
21. Altshuler G., Smirnov M., Yaroslavsky I. *J. Phys. D: Appl. Phys*, **38**, 2732 (2005).
22. Popov A.P., Priezzhev A.V., Lademann J., Myllylä R.A. *Kvantovaya Elektron*., **37**, 17 (2007) [*Quantum Electron*., **37**, 17 (2007)].
23. Lee S., McAuliffe D.J., Kollias N., Flotte, T.J., Doukas A.G. *Laser Surg. Med*., **31**, 207 (2002).
24. Menon G.K., Brandsma J.L., Schwartz P.M. *Skin Pharmacol. Physiol*., **20**, 141 (2007).
25. Kendall M., Rishworth S., Carter F., Mitchell T. *J. Invest. Dermatol*., **122**, 739 (2004).
26. Ossadnik M., Richter H., Teichmann A., Koch S., Schäfer U., Wepf R., Sterry W., Lademann J. *J. Biomed. Opt*., **16**, 747 (2006).
27. Belikov A.V., Altshuler G.B., Feldshtein F.I., Skripnik A.V., Shatilova K.V. http://bone-surgery.ru/view/m2..
28. Genina E.A., Bashkatov A.N., Korobko A.A., Zubkova E.A., Tuchin V.V., Yaroslavsky I.V., Altshuler G.B. *J. Biomed. Opt*., **13**, 021102 (2008).